

Probing Cool and Warm Infrared Galaxies using Photometric and Structural Measures

Nurur Rahman¹, George Helou, and Joseph M. Mazzarella

*Infrared Processing and Analysis Center/Caltech,
Mail Code 100-22, 770 S. Wilson Avenue,
Pasadena, CA 91125, USA*

nurur@ipac.caltech.edu; gxh@ipac.caltech.edu; mazz@ipac.caltech.edu

ABSTRACT

We have analyzed a sample of nearby cool and warm infrared (IR) galaxies using photometric and structural parameters. The set of measures include far-infrared color ($C = \log_{10}[S_{60\mu m}/S_{100\mu m}]$), total IR luminosity (L_{TIR}), radio surface brightness as well as radio, near-infrared, and optical sizes. In a given luminosity range cool and warm galaxies are considered as those sources that are found approximately 1σ below and above the mean color in the far-infrared $C - L_{TIR}$ diagram. We find that galaxy radio surface brightness is well correlated with color whereas size is less well correlated with color. Our analysis indicates that IR galaxies that are dominated by cool dust are large, massive spirals that are not strongly interacting or merging and presumably the ones with the least active star formation. Dust in these cool objects is less centrally concentrated than in the more typical luminous and ultra-luminous IR galaxies that are dominated by warm dust. Our study also shows that low luminosity early type unbarred and transitional spirals are responsible for the large scatter in the $C - L_{TIR}$ diagram. Among highly luminous galaxies, late type unbarred spirals are predominately warm, and early type unbarred and barred are systematically cooler. We highlight the significance of $C - L_{TIR}$ diagram in terms of local and high redshifts sub-millimeter galaxies.

Subject headings: galaxies: general - galaxies: spirals - galaxies: active - galaxies: starburst - galaxies: structure

¹National Research Council (NRC) Postdoc Fellow

1. Introduction

Observations by the *Infrared Astronomical Satellite (IRAS)* led to the identification of very luminous and ultra-luminous infrared galaxies, commonly known as the LIRGs and ULIRGs, respectively. These galaxies have enormous far-infrared (FIR) luminosities, $10^{11} < L_{FIR}/L_{\odot} < 10^{12}$ for LIRGs and $L_{FIR} > 10^{12} L_{\odot}$ for ULIRGs, and emit the bulk of their energy at the infrared wavelengths (Soifer et al. 1984, 1986, 1987; Sanders et al. 1988). Subsequent multi-wavelengths studies reveal that in the local universe ($z < 0.1$) ULIRGs have comparable total luminosities (L_{TIR}) and higher space densities than those of optical quasars (Sanders et al. 1988; Kim & Sanders 1998).

Understanding the nature and origin of energy sources in the LIRGs and ULIRGs has been the subject of much debate. Studies indicate that in the vast majority of these objects power comes from dust which is heated to various temperatures by various thermal and non-thermal processes such as ongoing (steady-state) star formation, intense starburst phase, and/or synchrotron radiation from the supernovae explosions (Lawrence et al. 1986; Genzel et al. 1998; Lutz et al. 1998). These systems may also be powered by active galactic nuclei (AGN; Lonsdale, Smith, & Lonsdale 1993). The energy distributions suggest that most of the observed FIR emission from luminous disk galaxies is due to the thermal radiation from warm dust heated by hot stars embedded in HII regions and molecular clouds heated directly by young OB stars; and cool dust from the general interstellar radiation field (Helou 1986; Presson & Helou 1987; Barvainis, Antonucci, & Coleman 1992). Dust could also be heated by shocks in the interstellar medium during the collision or interaction of galaxies (Harwit et al. 1987).

Dust heating mechanisms can be traced indirectly as each of these should correspond to particular spatial distributions of the FIR light. For example, the FIR emission originated by galaxies dominated by an AGN would appear compact and unresolved. On the other hand, starburst heated dust should have about the same scale size as the burst itself because young stars are well mixed with the gas from which stars are forming. Dust heated by the non-ionizing photons from cold, population I stars, might be expected to follow the smoothed distribution of older giants in the galaxy (Zink et al. 2000). A determination of the total energy output such as luminosity, the amount of dust present in the interstellar medium and its spatial distribution within the galaxies as well as its relationship to other basic components, such as the atomic and molecular gas, the stars, etc, is essential to studies connecting galactic structure and nature of the IR energy sources (Carico et al. 1990; Sopp & Alexander 1991, 1992; Andreani & Franceschini 1992, 1996; Alton et al. 1998; Domingue et al. 1999; Siebenmorgen, Krügel & Chini 1999; Haas et al. 2000; Stickel et al. 2000; Trewhella et al. 2000; Zink et al. 2000).

The FIR color C , defined by the *IRAS* 60 -to- 100 μm flux density ratio, an indicator of characteristic dust temperature, is a diagnostic of the typical heating conditions in the interstellar medium of a galaxy (Bothun, Lonsdale, & Rice 1989; Soifer & Neugebauer 1991). It has been shown that low-redshift *IRAS* galaxies exhibit positive correlation of C with L_{FIR} such that more luminous galaxies tend to be warmer as compared to less luminous galaxies (Soifer et al. 1987; Dale et al. 2001; see Fig.1 in this study). The color changes systematically over roughly three orders of magnitude in luminosity with large scatter. As a result there is a substantial number of highly luminous but cool galaxies as well as low luminosity yet warm/hot galaxies (Dale et al. 2001; Chapman et al. 2003). In this study we attempt to understand cool and warm IR luminous sources in terms of the geometric distribution of dust and galaxy morphology. In a given FIR luminosity range, these galaxies are considered in the context where cool galaxies are 1σ below and warm galaxies are 1σ above the mean color at a given luminosity. We are interested in differences between cool and warm galaxies in the same luminosity range that might suggest differences in the nature of the heating sources.

In an interesting study Young (1999) showed that star formation efficiency (SFE), defined by the ratio of L_{TIR} to molecular hydrogen mass M_{H_2} , anti-correlated with disk (optical) sizes. The trend is prevalent in galaxies of various Hubble types and environments. It has been attributed to the shear present in disk galaxies. The molecular clouds in larger disks would experience increased turbulence which would reduce the efficiency of star formation (Young 1999). Galaxies in Young’s sample span a broad range in FIR color comprising normal star forming galaxies (SFGs, $L_{FIR}/L_{\odot} < 10^{11}$) as well as LIRGs and ULIRGs. In Young’s study, however, it remains unexplored how cool and warm systems behave in the visual as well as in the longer wavelengths. Since the IR luminous galaxies contain very large amount of dust, the interpretation of any observation at optical or shorter infrared wavelengths gets complicated by extinction. Therefore, to probe the origin of large IR luminosity it is necessary to have the knowledge of the spatial extents of the emitting regions in observations unaffected by dust extinction.

The paper is organized as follows: we describe the data in §2 and parameter error estimation in §3. We present our results in §4 and discuss the implications of our results in §5. The conclusions are given in §6.

2. Data

IRAS resolved only the largest and nearest galaxies because of its comparatively large beam size of $\sim 2' - 4'$ at 60 and 100 μm . Therefore, the FIR brightness distributions of most

of the sources detected by the *IRAS* are unknown. In contrast to the rather large scatter in optical-FIR correlations, a tight correlation of FIR with radio continuum total flux densities for infrared-selected galaxies appear to hold locally within individual galaxies (Helou, Soifer & Rowan-Robinson 1985; Beck & Golla 1988; Bica, Helou, & Condon 1988; Murphy et al. 2006). In nearby galaxies where (*IRAS*) FIR sizes have been measured directly, radio sizes are known to match, or to be somewhat larger than the size scale in FIR (Bica & Helou 1990). Besides, FIR and radio continuum brightness distributions of these galaxies show remarkable similarity (Marsh & Helou 1995). The agreement in FIR and radio sizes, albeit derived from a smaller sample, suggest that high resolution radio maps may be taken as a good substitute, or at least as an upper limit for the size of the unobtainable FIR maps. We, therefore, use 1.49 GHz radio size as a proxy for the size of FIR emission.

Wang & Helou (1992, hereafter WH) studied the compactness of FIR bright galaxies and constructed a list of 330 galaxies from the *IRAS* Bright Galaxy Sample (BGS; Soifer et al. 1986, 1987, 1989). WH constructed a flux limited sample of extragalactic objects brighter than 5.24 Jy at 60 μm , covering the entire sky surveyed by the *IRAS* at galactic latitude $|b| > 30^\circ$. For radio data (rest frame flux density, size) WH used the atlas of the 1.49 GHz radio maps based on VLA observations of IR bright galaxies that had been compiled by Condon, Anderson & Helou (1990, hereafter CAH). After removing AGN dominated galaxies identified as highly compact radio sources, the final list of WH contained 218 galaxies. Our sample is based on this list of 218 galaxies. We use the same radio data, however, we take the rest frame *IRAS* flux densities, luminosity, and estimated distance of member galaxies from the Revised Bright Galaxy Sample (RBGS) since it provides the best available reference for accurate *IRAS* fluxes and IR luminosities of galaxies in the local universe (see Sanders et al. 2003 for details on RBGS).

Particular attention is given to exclude AGN from the sample. Although the list of WH was carefully compiled to get rid of the radio monsters, we have checked the entire sample following the prescription of de Grijp et al. (1985) using mid and far infrared color - color correlations. We have found 5 galaxies that fall into the region of the color - color plot which is mostly occupied by AGN like sources (de Grijp et al. 1985). We have removed them from the list. The radio fluxes of the remaining 213 galaxies correlate well with the *IRAS* fluxes, and all galaxies fall within $\sim 1.5\sigma$ of the mean q -value in the $L_{FIR} - q$ correlation indicating absence of radio excess objects (q parameter is defined in Condon, Anderson & Helou 1991). We have also made visual inspection of the observed spectral energy distributions of member galaxies. From this analysis we conclude that our final sample of 213 sources are star forming disk galaxies, although there may be AGNs present that are not energetically dominant in the far-infrared.

The number of SFGs, LIRGs, and ULIRGs in our sample are 154, 52, and 7, respectively. These three classes of galaxies have the following redshift distributions: $0.0 < z < 0.016$, $0.012 < z < 0.051$, and $0.018 < z < 0.082$ with the median redshifts 0.006, 0.023, and 0.055. The effective color temperature of the integrated dust emission in the sample galaxies ranges in between $\sim 25K - 40K$, assuming emissivity index, $\beta = 2$ (Dunne et al. 2000; Dunne & Eales 2001). The ULIRGs show signs of interaction, e.g., presence of neighbor and accretion, e.g., tidal tails and disturbed outer envelopes. Majority of LIRGs appear as single, isolated systems while 30% of them appear disturbed. At the lower end of the luminosity range, the LIRGs are luminous single isolated galaxies, with features resembling to the low luminosity SFGs. A minority of SFGs (15%) has disturbed outer envelope or nearby companion.

The NASA/IPAC Extragalactic Database (NED) and the Lyon-Meudon Extragalactic Database (LEDA) has been used to obtain Galactic extinction corrected B -band luminosity L_B and 25 mag arcsec⁻² linear diameter D_B . The near-infrared (NIR) K_s band ($2.17\mu m$) magnitude of our sample is $5.0 < K_s < 10.6$. For bright galaxies Jarrett et al. (2000) have recommended K_s band 20 mag arcsec⁻² diameter D_{NIR} as the most reliable and robust for galaxy photometry. We obtain D_{NIR} from Two Micron All Sky Survey catalog (Jarrett 2000) using a 5'' search radius. We did not find any reliable B -band size for CGCG247-020, IRASF 08339+6517, and IRASF 12132+5313, and NIR size for NGC 5256, NGC 5331, and MCG+07-23-019. All these galaxies belong to the LIRGs sub-sample. No correction was applied to the luminosities and diameters for internal extinction or inclination of the host galaxies. Following RBGS we adopt $\Omega_M = 0.3$, $\Omega_\Lambda = 0.7$, and $H_0 = 75$ km sec⁻¹ Mpc⁻¹. These values are slightly different than recent estimates from Wilkinson Microwave Anisotropy Probe (WMAP; Spergel et al. 2003). Table 1 includes a partial list of low luminosity star forming galaxies showing only cool and warm sources. In the table galaxies are sorted in ascending order of FIR color, i.e. galaxy numbered 1 has the lowest FIR color, for all luminosity classes [*See the electronic edition of the Journal for the complete list of galaxies*].

3. Uncertainty in Parameters

We use L_{TIR} as a photometric measure, instead of L_{FIR} , since the former is based on the all four fluxes measured by the *IRAS* and thus taking contributions from almost the entire IR range (Sanders & Mirabel 1996). The median uncertainties associated with the *IRAS* flux densities are $\sim 5\%$ and $\sim 3\%$ at 12 and 25 microns, respectively, and $\sim 1\%$ in both far-infrared bands. This leads to a 2% uncertainty in the FIR color of a galaxy which is much smaller than the spread in mean color in a given luminosity. The total IR flux of

a galaxy is a weighted sum of four *IRAS* flux densities. With the corresponding weighting factors given in Sanders & Mirabel (1996) the median uncertainty in the total IR flux of a galaxy is $\sim 1\%$.

Distances for the galaxies are taken from the RBGS. Most of the RBGS distance estimates come from redshift measurements, application of the Hubble law and correction for the Mould et al. (2000) flow model. However, some are primary (P) or secondary (S) distance estimates as flagged in the RBGS Table 1 which do not come from the Hubble flow and cosmic attractor model. Our sample contains 48 galaxies of such distance estimates, all of which belong to the SFGs sub-sample. A significant uncertainty to a galaxy size and L_{TIR} would result from an uncertainty in the distance estimate. Surface brightness being the distance independent measure would not be affected. The observed heliocentric radial velocities of sample galaxies are measured $\sim 1 - 2\%$ accuracy (obtained from NED). The uncertainties associated with the model parameters such as motions in the Local group, Virgo centric infall, Great Attractor infall etc. are high ($\geq 10\%$; Mould et al. 2000). The uncertainty associated with other distance estimates is of similar magnitude. A galaxy optical angular size has less than 10% uncertainty, depending on the flattening of the disk, as given in the Third Reference Catalog (de Vaucouleurs et al. 1991; RC3). We assume a similar uncertainty in the NIR and radio bands (we note that it varies in different bands). Combining all of the preceding, we assign $\sim 15\%$ and $\sim 20\%$ uncertainty, respectively, to the estimate of physical size and L_{TIR} of a galaxy.

The uncertainty in 1.49 *GHz* surface brightness is due to the measurement errors in 1.49 GHz flux density and angular size. According to CAH (1990), the contributions from rms confusion error and calibration error to the 1.49 *GHz* flux density are smaller than the noise error. The rms radio map noise σ_n is between 0.1 and 0.2 mJy per beam solid angle $\Omega_b \sim \theta_{beam}^2$ (Condon 1987; CAH 1990). The noise contribution to the flux density is $\sigma_S \approx \sigma_n(\Omega/\Omega_b)^{1/2}$ in mJy, where $\Omega \sim \theta_M^R \times \theta_m^R$ is the solid angle covered by the source and θ_M^R, θ_m^R are the deconvolved major (*M*) and minor (*m*) axes of a radio image. Radio maps in CAH (1990) ranges in FWHM angular resolution from 1.5'' to 60'' depending on the source's apparent size. Using $\sigma_n = 0.2$ mJy for each galaxy gives an uncertainty of $\sim 2\%$ in 1.49 *GHz* flux density. Uncertainty in radio size varies with beam resolutions but it is within 5% in all cases. Taking this upper limit we find $\sim 10\%$ uncertainty in the surface brightness coming from 1.49 *GHz* flux density and angular size.

4. Results

Figure 1 shows the FIR color - IR luminosity diagram for *IRAS* $S_{60\mu m} > 1.2$ Jy sample of ~ 4700 sources (Fisher et al. 1995) in panel a and our sample of 213 galaxies with $S_{60\mu m} > 5.4$ Jy in panel b. The former sample is shown after removing 330 spurious cold luminous galaxies as pointed out by Chapman et al. (2003). In both panels horizontal bar and small cross represent median, and mean color with 1σ error bar. These panels highlight the fact that galaxy FIR color and total IR luminosity follow a broad correlation with large spread in different flux limited samples. In this figure small triangles and dots represent SFGs and LIRGs, respectively (Fig.1b). For these two classes of galaxies solid symbols represent cool sources (around or below 1σ from the mean C) and open symbols represent the warm sources (around or above 1σ from the mean C). Open stars are used for the ULIRGs. Because of their limited number we are unable to separate these ultra-luminous galaxies into cool and warm categories. In this panel large crosses represent local sub-millimeter galaxies (see below for a discussion of these galaxies).

Figure 2 shows color as a function of $SB_{1.49GHz}$ as well as galaxy size in radio, NIR, and optical bands. The choice of these parameters are based on conventional practice which suggests that radio size is a stand-in for FIR emission size, NIR size represents emission from old stellar population, and optical size accounts for the emission from a mixture of both young and old stars but complicated by dust. We have used the major axis to estimate the area of each object to reduce the effects of highly uncertain inclinations. The radio surface brightness is calculated as $S_{1.49GHz}/(\theta_M/2)^2$.

Cool and warm galaxies separate clearly in the surface brightness vs. color diagram (Fig.2a). For each luminosity class, warm colors correlate with high surface brightness. Panel b indicates that galaxies that are dominated by cool dust are large, massive spirals that are not strongly interacting or merging and presumably the ones with the least active star formation. Dust in these cool objects is also, on average, less centrally concentrated than in the more typical LIRGs and ULIRGs that are dominated by warm dust. There is a clear sequence in the progression of color with radio size: color increases systematically from normal/isolated disks toward merger/disturbed disks. The latter type of disks are shown by asterisk symbols. Panels a and b shows that color is strongly correlated with both surface brightness and galaxy size at $1.49 GHz$ (see Table 2 for correlation statistics). Note that the uncertainty in color or brightness is statistical in nature and do not include calibration error. However, it will not affect our results since incorporating calibration error will simply shift these physical parameters systematically.

The statistical trend in Fig.2b and Fig.2c suggests that luminous cool galaxies, where older stars have greater spatial distribution, show a tendency to have cool dust distributed

over larger volume. This may be interpreted, as an indirect but interesting support, that FIR light from cool galaxies are reprocessed emission of photons coming predominantly from the old population of stars. This is in accord with the expectation that dust heated by the non-ionizing photons from a cooler population of stars might follow the smoothed distribution of older stars in the galaxy. In spite of a large scatter, we can see a moderate trend where warm sources have relatively smaller regions of NIR emission than their cool counterparts. Most of the ULIRGs (4/7) have larger NIR and B -band diameters than found among warm ($C > -0.2$) LIRGs (Fig.2c and 2d). It is interesting that ULIRGs, which all have very warm dust ($C > -0.1$), have NIR and B diameters comparable to the subset of LIRGs with relatively cool dust temperatures ($C < -0.22$). The data indicate that the ULIRGs have relatively large disks (e.g., they involve mergers of massive galaxies) with compact cores that dominate the FIR emission. It is also clear from Fig.2c that warm LIRGs (large open circles) have systematically smaller NIR diameters than cool LIRGs (large solid circles). We conclude that some galaxies with relatively cool dust temperatures are LIRGs (rather than lower luminosity SFGs) because, despite having a lower average SFR per unit area, they have on average larger total surface areas than warm LIRGs.

The Optical size, representing the spatial distribution of stellar emission, shows no trend with the color when the whole sample is considered (Fig.2d). However it improves for SFGs+LIRGs, after removing ULIRGs from the sample (see Table 2 for correlation statistics). The scatter is large as compared to Fig.2b and Fig.2c. All ULIRGs and a substantial number of warm SFGs and LIRGs are almost similar in optical size compared to their cool counterparts. All of these warm sources show signs of interaction such as tidal tail, disturbed outer region or presence of neighbors.

With the exception of color and $SB_{1.49GHz}$ all of the physical parameters depend on the distance. Figure 2 demonstrates that color is tightly correlated with distance independent measures. On the other hand correlation between color and galaxy size is weak. There are at least three factors that can contribute to the broader distribution in color-size correlations (see Table 2 for correlation statistics). First, there may be large error in the distance measurement in spite of correction for non-Hubble flows since correlation between color vs. NIR or B-band surface brightness is relatively stronger compared to the respective sizes. Second, optical diameter D_B of interacting/merging galaxies will overestimate the actual size because of the inherent difficulty associated with size estimates of these sources. Removing the ULIRGs from the sample makes the color-size trend stronger. Third, varying scatters in color vs. size plots reflect methodological differences in estimating angular size in different wavelengths. The scatter would have been reduced if galaxy sizes were estimated in all wavelengths in a systematic manner, e.g., at the same brightness level.

Figure 3 shows color as a function of galaxy (optical) morphology. We use RC3 classification and divide galaxies into three broad categories: unbarred (A), transitional (AB), and barred (B). In each morphology bin, we take S0?-S0a-Sa-Sb-Sbc sources as early type, and S?-Sc-Scd-Sd-I-Pec sources as late type. Early and late type division is made to be consistent with earlier studies that have found fundamental differences in the properties of early and late type galaxies, especially, barred galaxies (Combes & Elmagreen 1993; Ho, Filippenko & Sargent 1997; Sakamoto et al. 1999; Sheth et al. 2005).

We did not find any classification for 11 LIRGs and it is also uncertain for the seven ULIRGs [*See Table 1 in the electronic edition of the Journal for these galaxies*]. As a result, Fig.3 shows 154 SFGs and 41 LIRGs divided into SA, SAB, and SB type sources. This figure illustrates that high luminosity LIRGs are mostly unbarred spirals (Fig.3a, b). The transitional and barred spirals, in general, fall into the class of low luminosity SFGs (Fig. 3c,d and e,f). The essence of this figure are the followings: for SFGs, late type spirals stay close to the mean color (Fig.3d and f). Early type spirals, on the other hand, are responsible for the scatter in color-luminosity diagram (Fig.3a, c, and e). Interestingly, cool sources consist of early type unbarred and transitional galaxies whereas warm sources consist of early types of all three categories. In other words, low luminosity barred galaxies, in general, show a tendency to have higher color temperature. For LIRGs, late type unbarred galaxies are predominately warm (Fig.3b). This is not unexpected since late type galaxies are highly irregular systems with higher star formation rate which results in warmer color. Early type LIRGs are systematically cooler (Fig.3a, c, and e). Both transitional and barred spirals are extremely rare in this luminosity class.

In a recent study, Sheth et al. (2005) showed that late types barred spirals are less centrally concentrated than early types and a significant subset of early type barred spirals have little or no gas within the bar region. This observation has been explained as a result of higher mass accretion rates in the past in early type barred spirals where the large amount of gas driven inward by the bar have already been converted into stars. They suggested that these galaxies are in the post-starburst phase. The IR luminosity of Sheth et al. sample of 44 galaxies span the range, $10^9 < L_{TIR}/L_{\odot} < 10^{11}$, which we call star forming galaxies (SFGs) in our sample. These galaxies fall in the class of SFGs in our sample. The observation that early type barred spirals are in the post-starburst phase gives a plausible explanation for these galaxies to be low luminosity star forming systems.

Note that the RC3 classifications used here are based on optical images that are strongly affected by dust obscuration in our FIR-selected galaxy sample. More recent studies at NIR wavelengths indicate the presence of stellar bars in a large fraction of disk galaxies that appear unbarred at optical wavelengths (Eskridge et al. 2000). In addition, when one extends the

bar detection sensitivity to a low relative amplitude of $\sim 3\%$ in the K band, nearly 90% of a sample of optically unbarred (SA) spirals contain stellar bars (Grosbol, Patsis, & Pompei 2004). Therefore, the fractions of transition (SAB) and barred (SB) galaxies is likely to be much higher than is indicated by the RC3 classifications, and the optical bar fractions may be telling us more about the relative extinction by dust at optical wavelengths than the intrinsic stellar distributions. An improved understanding of this issue requires detailed analysis of near-IR images for a large sample of LIRGs and ULIRGs.

5. Discussions

It is necessary to address whether the large scatter in the FIR color-luminosity diagrams is real (intrinsic to the physics of the objects), or an artifact of the observations. Figure 1 shows the data from the IRAS sample of Fisher et al. ($S_{60\mu m} > 1.2$ Jy; panel a) and data from the RBGS ($S_{60\mu m} > 1.2$ Jy; panel b). The main objective of the RBGS was to produce more accurate fluxes for the many large, nearby galaxies resolved by IRAS, by recovering extended emission that was not represented in the (underestimated) flux densities reported for such objects in the IRAS Point Source Catalog (PSC) and Faint Source Catalog (FSC). The RBGS also added some objects missed in the previous BGS compilations. This problem is minimal for the fainter objects in the 1.2 Jy sample, which on average are more distant and therefore smaller than the RBGS objects, with little or no flux missed in the published PSC/FSC flux densities. The main conclusion we can draw from comparing Fig. 1a with Fig. 1b is that the scatter in the 5.24 Jy RBGS is consistent with the scatter in the Fisher et al. 1.2 Jy sample. The presence of more true statistical outliers ($\geq 3\sigma$ in each luminosity bin) in the 1.2 Jy sample compared to the 5.24 Jy sample is expected from basic sampling statistics, as is the extension to higher L_{TIR} values due to sampling of a much larger volume of space in the 1.2 Jy sample. As stated in previous sections, the uncertainty in the L_{TIR} values are dominated by the distance determinations ($\sim 15\%$), and the uncertainty in C is relatively small (See the representative error bar in Fig. 1a). Therefore, we conclude that the dispersion in the $C - L_{TIR}$ diagram is intrinsic and related to the diversity of physical conditions of the ISM in the galaxies.

To understand the physical origin of the color-luminosity diagram it is necessary to have detailed knowledge of these cool and warm galaxies. Questions can be raised such as, in a given luminosity range, what are the possible (external or internal) mechanisms that would cause some galaxies to have cool color temperature compared to the majority of the galaxies? what are the basic connections between the photometric and structural properties of galaxies in this diagram? We proceed in light of above queries and find that dust in the

cool objects is less centrally concentrated than in the more typical LIRGs and ULIRGs that are dominated by more centrally concentrated warm dust. We also find that the optical disks of IR cool galaxies show a tendency to be more extended than those of the warmer ones. The color-size trend is relatively stronger at longer wavelengths. The extended emission in cool sources may well indicate heating by old stars, but it could also indicate simply wide-spread small star forming regions scattered in a large dusty disk. Distinguishing between these aspects is beyond the scope of this study.

The color-luminosity trend shown in Figure 1 is observed in the local universe ($z < 0.082$). It had been demonstrated that the trend does not change out to $z \sim 1$ (Chapman et al. 2003) meaning that the dispersion of color in each luminosity bin does not vary significantly with redshift. However, given the presence of higher luminosity objects such as hyper-luminous galaxies with $L_{TIR}/L_{\odot} > 10^{13}$ in high-redshift samples that cover much larger volumes of space and earlier look-back times than local samples, from the present data we can only make such inferences for objects with $L_{TIR}/L_{\odot} \leq 10^{12.5}$. In this respect, this correlation, therefore, reveals something quite profound: in absence of any structural information of high z luminous galaxies we can get a rough idea about the extent of the disks if we simply know the FIR colors and luminosities of these galaxies. In spite of a large scatter, the trend suggests that cool galaxies are generally highly luminous because of extended disks. The warm galaxies may or may not have extended disks depending on galaxy environment and/or internal processes.

Current sub-millimeter/millimeter (sub-mm/mm) surveys have discovered a new population of $z > 1$ sub-mm galaxies, contributing up to 50% of the extragalactic background light (Smail, Ivison, & Blain 1997; Barger et al. 1998; Hughes et al. 1998; Borys et al. 2003). There are two possible explanations of these galaxies: they are either proto-spheroids with high star formation rate $\geq 10^3 M_{\odot} \text{ yr}^{-1}$ (Dunlop 2001) or disks dominated in the sub-millimeter by infrared cirrus heated by their interstellar radiation field, rather than intense star formation (Rowan-Robinson 2001; Efstathiou & Rowan-Robinson 2003, hereafter ERR; King & Rowan-Robinson 2003). ERR have modeled cirrus emission for a selection of local ($z < 0.02$) and high- z (> 1) sub-mm galaxies and found excellent agreement in all cases. Their work suggests that sub-mm count and background can be understood in terms of cirrus-like emission (with effective dust temperature < 30 K) rather than invoking dusty ultraluminous starburst galaxies, e.g. Arp 220 in our local universe, to be the representative of distant sub-mm galaxies. The significance of ERR work is that if the cool component dominates the observed sub-mm fluxes of these high- z sub-mm/mm wave survey sources the emission should be extended rather than compact (i.e. centrally condensed). We attempt to explore this aspect of sub-mm galaxies in the context of our study by analyzing the 1.49 GHz emission of the local sample of ERR since only these galaxies are available in the RBGS.

The local sample of ERR includes UGC 0903, NGC 0958, NGC 1667, NGC 2990, UGC 5376, NGC 5962, NGC 6181. We remove NGC 2990 from the ERR sample because it has $S_{60\mu m} < 5.24$ Jy placing it below the flux limit of the RBGS. Except NGC 1667 and UGC 5376, the other four galaxies are present in our sample. The IR and radio information of these two galaxies are obtained respectively from the RBGS and the NRAO VLA Sky Survey catalog (NVSS; Condon et al. 1998). The FIR color and total IR luminosities of these six galaxies (shown by large crosses) are similar to normal SFGs and cool LIRGs in our sample (Fig.1b). We find that these galaxies indeed have large radio (FIR) disks. The 1.49 GHz radio source diameters of these galaxies range ~ 4 to 20 kpc, which is comparable to cool LIRGs and even normal SFGs (those not defined in this study as unusually cool or warm). This is in stark contrast to the warm SFGs and LIRGs that have radio sizes less than ~ 3 kpc (See Fig.2b).

The FIR cool high- z sub-mm galaxies of ERR sample carry a few $\times 10^{13} L_{\odot}$, several hundred times more luminosity than these local examples. Assuming that these galaxies are scaled-up versions of local cool examples, where disk size increases at constant surface brightness to account for the increased luminosity, we find that their radio (and FIR) disks must range up to 100 kpc or more in size. While rare, local galaxies with similar sizes do exist, as in the case of low surface-brightness, HI-rich galaxies (Sprayberry et al. 1995; Bothun, Impey, & McGaugh 1997; Matthews, van Driel, & Monnier-Ragaïn 2001). At earlier epochs the cool sub-mm galaxies may be single large disks able to regulate their star formation at the modest level required for these luminosities and FIR colors. But what do we know from observations about the extent of FIR/Radio emission in these distant sub-mm sources, especially the FIR cool ones ?

For the assumed cosmology in this study, the linear disk size of 100 kpc corresponds to an angular size of $> 7''$ for $z > 1$ sub-mm galaxies. On the other hand, the reported sizes of sub-mm galaxies in the redshift range $1 \lesssim z \lesssim 4$ are significantly smaller, $\lesssim 1.5$ (Ivison et al. 2002; Iono et al. 2006; Tacconi et al. 2006). This suggests that the objects measured are best understood as scaled-up versions of local FIR warm ULIRGs rather than cool extended disks (Tacconi et al. 2006), since nothing is known about their FIR colors. While cold ULIRGs had been detected in the redshift range $0.4 < z < 1$, very little is known about their morphology or geometry (Chapman et al. 2002). However, the recently reported optical properties of BzK-15504 (Genzel et al. 2006) make it a very likely FIR cool luminous galaxy. At $z = 2.38$, its disk extends out to ~ 10 kpc, and has elevated distributed star formation throughout in addition to an accreting central black hole. The estimated total star formation rate for this galaxy is $140_{-80}^{+100} M_{\odot} \text{ yr}^{-1}$ (Genzel et al. 2006) suggesting that it is an ultra-luminous infrared galaxy with $L_{TIR} \gtrsim 10^{12} L_{\odot}$.

The relative frequency of occurrence of FIR cool objects as a function of redshift is still unknown, and the detection efficiency will decrease as the source extent increases. Tacconi et al. have measured 8 objects, all of which were compact. Their results only place a limit on the effective dust temperature (39 ± 3 K for $\beta = 1.5$) of sub-mm galaxies rather than the frequency of cool objects. As precise redshifts and more accurate rest frame FIR fluxes of high- z galaxies become available, placing these sub-mm/mm galaxies in the context of the FIR color-luminosity diagram will help shed light on their structure. Combining that with kinematic information may constrain further the nature and evolving path of these galaxies.

Warm LIRGs and ULIRGs are usually associated with intense bursts of star formation. These galaxies are known to have higher star formation rates (SFR) and star formation efficiency (SFE) than lower luminosity galaxies. These parameters are defined in such a manner that the SFR is directly related to the L_{TIR} (Kennicutt 1998) whereas the SFE is the L_{TIR} normalized by the molecular hydrogen mass (Young 1999). It has been noted that along the Hubble sequence, the SFR increases toward late-type, which could be due to dynamical instability increasing with decreasing bulge-to-disk ratio (Combes 2001). This trend is generally observed among the optically unbarred spirals in the present study as well, whereas galaxies with warmer FIR colors and hence higher SFRs are less likely to be transitional (SAB) or barred (SB) galaxies (See Fig.2)

Question can also be raised such as, what types of morphological features do the cool and warm galaxies have and how could these features be linked with the FIR color-luminosity correlation? We find that the LIRGs in our sample are mostly late type unbarred spirals. The transitional and barred spirals, in general, fall into the class of low luminosity SFGs. Among LIRGs, the late type unbarred spirals are predominately warm, and the early type unbarred and barred are systematically cooler. One probable reason for the transitional and barred spirals being low luminosity star forming galaxies is that they are in the post-starburst phase, where the large amount of gas driven inward by the bar have already been converted into stars, consistent with the findings of Sheth et al. (2005).

Finally we note that the low luminosity early type unbarred (SA) and transitional (SAB) spirals are responsible for the large scatter in the $C - L_{TIR}$ diagram. It may be that, in spite of our selection process, we have dust enshrouded AGN in the sample. These sources could span the entire luminosity range considered and could contribute to the scatter in this diagram. On the other hand this scatter may also arise from more variability in the SFR and star formation behavior, e.g., short episodic starburst or more possible configurations, e.g., large bulges and small star formation disks of early type sources.

6. Conclusions

We have analyzed a sample of 213 nearby IR galaxies to study the correlations of galaxy FIR color vs. several photometric and physical parameters. The set of measures include total IR luminosity, radio surface brightness as well as radio, NIR, and optical sizes. Our objective is to understand cool and warm IR sources using various correlations. We find that galaxy radio surface brightness is well correlated with FIR color whereas size is less well correlated with color. A weak color-size correlation signals a significant uncertainty associated with the distance measurements of sample galaxies. It may also reflect methodological differences in estimating angular size in different wavelengths. We also find that late type galaxies (from Sc and beyond) of all morphology classes show less scattering than early types in the color-luminosity diagram. Our study shows that dust in the cool IR sources is probably less centrally concentrated than in the more typical luminous and ultra-luminous IR galaxies that are dominated by more centrally concentrated warm dust. We believe this result has significant implication in terms of FIR color-luminosity diagram: in absence of any structural information of high- z luminous sources one can get rough estimate of the extent of the disks if one simply knows the FIR colors and luminosities of galaxies.

We thank the referee Jim Houck for insightful comments, and Thomas Jarrett for many useful communications. NR thanks Ranga Ram Chary, Roc Cutri, Justin Howell, Guilain Lagache, Seppo Laine, Naveen Reddy, Kevin Xu, Min Su Yun, Zang Wang for discussions. NR gratefully acknowledges the support of a Research Associateship administered by the National Research Council (NRC; upto December, 2005) and currently by the Oak Ridge Associated Universities (ORAU) during this research. This study has made use of the NASA/IPAC Extragalactic Database (NED) which is operated by the Jet Propulsion Laboratory, California Institute of Technology, USA under contract with the National Aeronautics and Space Administration, and the LEDA database in France.

REFERENCES

- Andreani, P. & Franceschini, A. 1996, MNRAS, 283, 85
- Andreani, P. & Franceschini, A. 1992, A&A, 260, 89
- Barger, A. J., Cowie, L. L., Sanders, D. B., Fulton, E., Taniguchi, Y., Sato, Y., Kawara, K., & Okuda, H. 1998, Nat, 394, 248
- Barvainis, R., Antonucci, R., & Coleman, P. 1992, ApJ, 399, L19

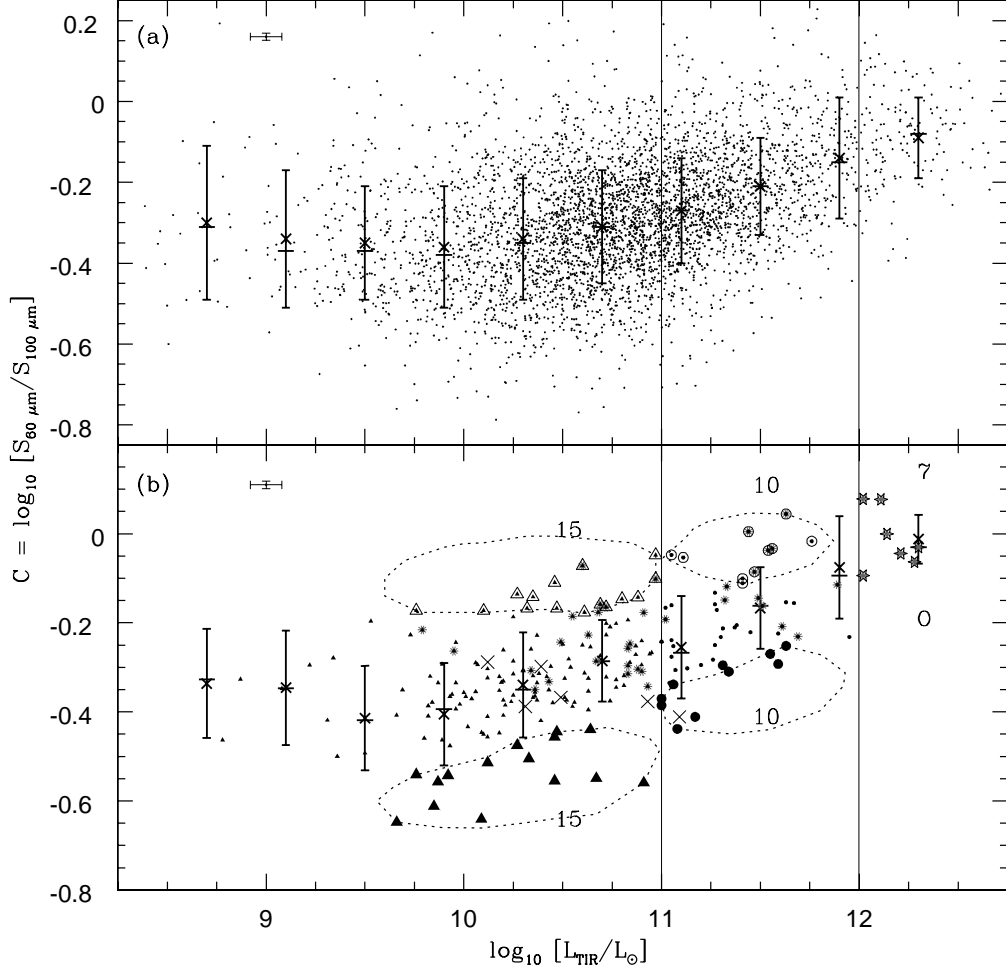


Fig. 1.— FIR color as a function of L_{TIR} for the *IRAS* $S_{60\mu m} > 1.2$ Jy sample of ~ 4350 galaxies (panel a), and our sample of 213 galaxies (panel b). Three classes of galaxies, in general, are shown by small triangles (SFGs), small dots (LIRGs), and stars (ULIRGs). The cool and warm sources are indicated, respectively, by large filled symbols and open symbols (triangles for SFGs and circles for LIRGs) in the regions delineated by dotted closed curves. In each luminosity bin the horizontal bar and (small) cross represent median and mean color. Each luminosity class (delineated by long vertical lines) contains equal number of cool and warm sources: 15+15 for SFGs and 10+10 for LIRGs. Large crosses and asterisks represent, respectively, local sub-mm and interacting/disturbed galaxies. A representative error bar is shown at the top of each panel.

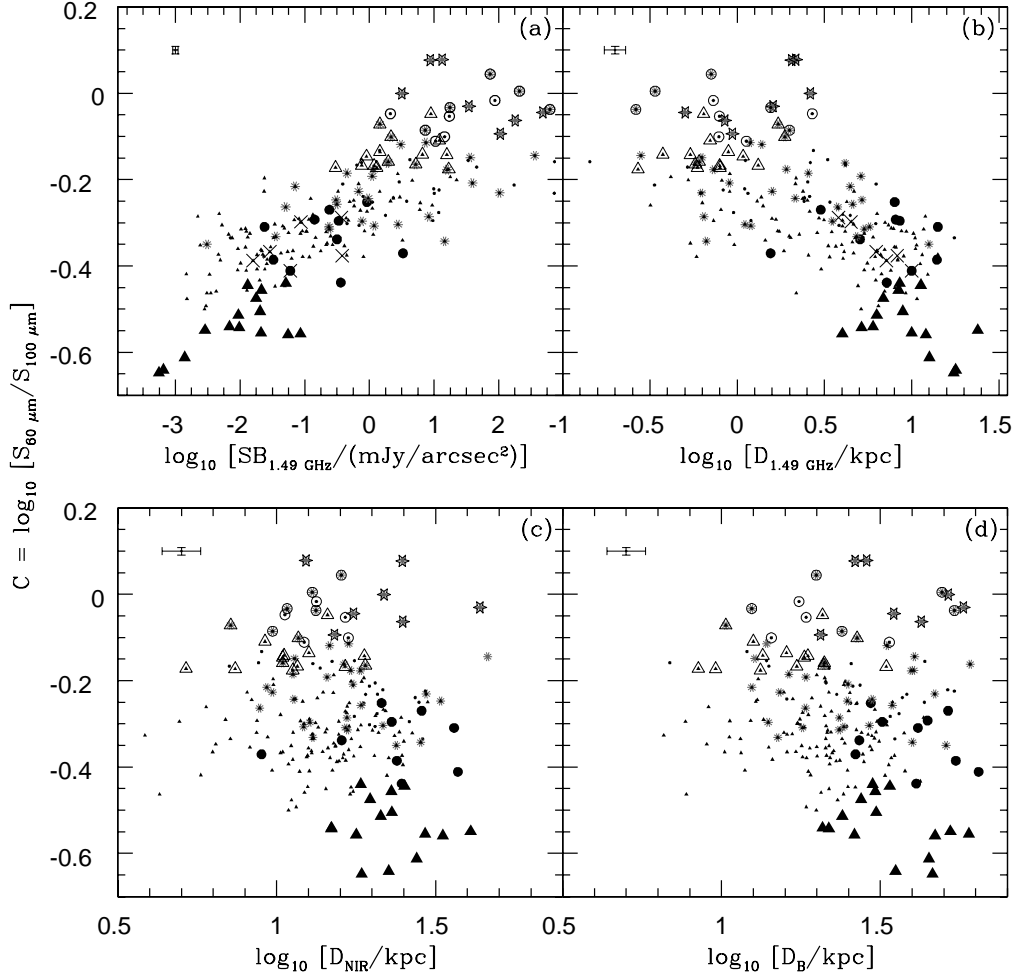


Fig. 2.— FIR color as a function of radio surface brightness (panel a), radio size (panel b), NIR size (panel c), and optical size (panel d). In each luminosity class cool sources have smaller surface brightness than the warmer ones (panel a). The FIR/Radio emission in the cool systems are extended over larger area compared to the warmer one where the emission is more compact (panel b). A weak trend between cool and warm sources can also be noticed in the NIR and visual bands (panels c and d). Large crosses (in panels a and b) and asterisks represent, respectively, local sub-mm and interacting/disturbed galaxies. The symbols used are the same as in Fig. 1. A representative error bar is shown at the top left in each panel.

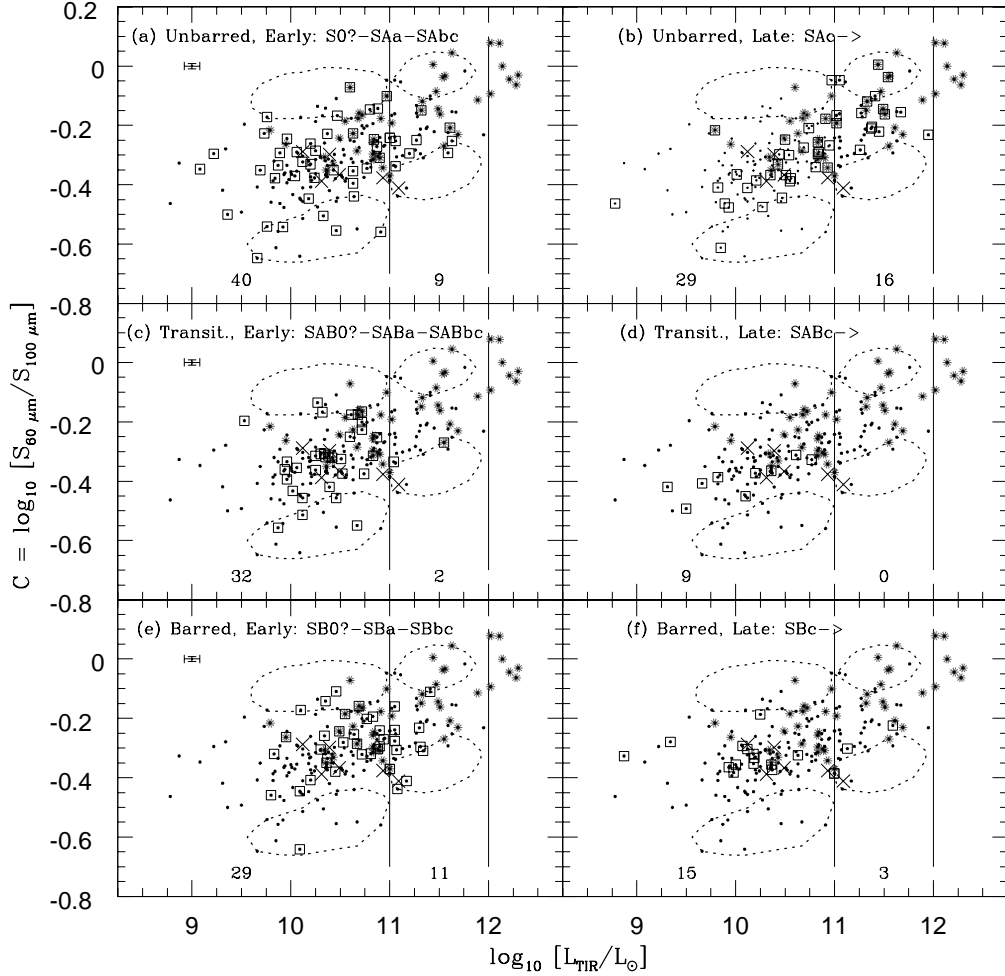


Fig. 3.— FIR color as a function of galaxy (optical) morphology. Dotted closed curves show the regions of cool and warm sources. Large crosses and asterisks represent, respectively, local sub-mm and interacting/disturbed galaxies. Representative error bar is shown at the top left and the number of galaxies with different morphologies are shown at the bottom of each panel. Only those galaxies, 154 SGFs and 41 LIRGs, that have morphological classification available in RC3 catalog are shown. Note from the figure that both transitional and barred spirals appear to be low luminosity star forming galaxies whereas high luminosity warm galaxies are predominantly unbarred (i.e. normal spirals). Cool and warm sources, in a given luminosity class, contain spirals with various morphologies.

- Beck, R. & Golla, G. 1988, *A&A*, 191, L9
- Bicay, M. D. & Helou, G. 1990, *ApJ*, 362, 59
- Bicay, M. D., Helou, G., & Condon, J. J. 1988, *ApJ*, 338, L53
- Bothun, G. D., Impey C. D., & McGaugh, S. S. 1997, *PASP*, 109, 475
- Bothun, G. D., Lonsdale, C. J., & Rice, W. 1989, *ApJ*, 341, 129
- Borys, C., Chapman, S. C., Halpern, M., & Scott, D. 2003, *MNRAS*, 344, 385
- Carico, D. P., Sanders, D. B., Soifer, B. T., Matthews, K., & Neugebauer, G. 1990, *AJ*, 100, 1
- Chapman, S. C., Helou, G., Lewis, G. F., & Dale, D. A. 2003, *ApJ*, 588, 186
- Chapman, S. C., Smail, I., Ivison R. J., Helou, G., Dale, D. A., & Lagache, G. 2002, *ApJ*, 573, 66
- Combes, F. 2001, in *ASP Conference Series Vol. 249, The Central kpc of Starburst and AGN*, ed. Knapen, J. H., Beckman, J. E., Sholsman, I., & Mahoney, T. J. (San Francisco: ASPC) 475
- Combes, F., & Elmagneen, B. G. 1993, *A&A*, 271, 391
- Condon, J. J. 1987, *ApJS*, 65, 485
- Condon, J. J., Anderson, M. L., & Helou, G. 1991, *ApJ*, 376, 95 (CAH)
- Condon, J. J., Cotton, W. D., Greisen, E. W., Yin, Q. F., Perley R. A., Taylor, G. B., & Broderick, J. J. 1998, *AJ*, 115, 1693 (NVSS)
- de Grijp, M. H. K., Miley, G. K., Lub, J., & de Jong T. 1985, *Nature*, 314, 240
- de Vaucorleurs, G., de Vaucorleurs, A., Corwin, H. G., Buta, R. J., Peturel, G., & Fouque, P. 1991, *Third Reference Catalog of Bright Galaxies* (New York: Springer) (RC3)
- Dale, D., Helou, G., Contursi, A., Silbermann, N. A., & Kolhatkar, S. 2001, *ApJ*, 549, 215
- Domingue, D. L., Keel, W. C., Ryder, S. D., & White, III R. E. 1999, *ApJ*, 118, 1542
- Dunlop J., 2001 in *Proc. UMass/INAOE Conf., Deep Milimeter Surveys: Implications for Galaxy Formation and Evolution*, ed. Lowenthal, J. D., & Hughes D. H. (World Scientific, Singapore) 11

- Dunne, L., & Eales, S. 2001, MNRAS, 327, 697
- Dunne, L., Eales, S., Edmunds, M., Ivison, R., Alexander, P., & Clements, D. L. 2000, MNRAS, 315, 115
- Efstathiou, A., & Rowan-Robinson, M. 2003, MNRAS, 343, 322 (ERR)
- Eskridge, P. B. et al. 2000, AJ, 119, 536
- Fisher, K. B. et al., 1995, ApJS, 100, 69
- Genzel, R. et al. 2006, Nature, in press, astro-ph/0608344
- Genzel, et al., 1998, ApJ, 498, 579
- Grosbol, P., Patsis, P. A., & Pompei, E. 2004, A&A, 423, 849
- Haas, M., Klass, U., Coulson, I., Thommes, E., & Xu, C. 2000, A&A, 356, L83
- Helou, G., Khan, I. F., Malek, L., & Boehmer L. 1988, ApJS, 68, 151
- Helou, G. 1986, ApJ, 311, L33
- Helou, G., Soifer, B. T., & Rowan-Robinson, M. 1985, ApJ, 298, L7
- Ho, L. C., Filippenko, A. V., & Sargent, W. L. W. 1997, ApJ, 487, 591
- Hughes, D. H. et al., 1998, Nature, 394, 241
- Ivison R. J. et al. 2002, MNRAS, 337, 1
- Iono D. et al. 2006, ApJ, 640, L1
- Jarrett, T. H. 2000, PASP, 112, 108
- Jarrett, T. H., Chester, T., Cutri R., Schneider, S., Skrutskie, M., & Huchra, J. P. 2000, AJ, 119, 2498
- Kennicutt, R. C. 1998, ApJ, 498, 541
- Kim, D. C., & Sanders, D. B. 1998, ApJSS, 119, 41
- King, A. J., & Rowan-Robinson, M. 2003, MNRAS, 339, 260
- Lawrence, A., Walker, D., Rowan-Robinson, M., Leech, K. J., & Penston, M. V. 1986, MNRAS, 219, 687

- Lonsdale, C., Smith, H., & Lonsdale, C. 1993, ApJ, 405, L9
- Lutz, D., Spoon, H. W. W., Rigopoulou, D., Moorwood, A. F. M., & Genzel, R. 1998, ApJ, 505, 103
- Marsh, K. A., & Helou, G. 1995, ApJ, 455,
- Matthews, L. D., van Driel, W., & Monnier-Ragaine, D. 2001, A&, 365, 1
- Mould, J. R., et al. 2000, ApJ, 529, 786
- Murphy, E. J., et al. 2006, ApJ, 638, 157
- Persson, C. J., & Helou, G. 1987, ApJ, 314, 513
- Rowan-Robinson, M. 2001, ApJ, 549, 745
- Sakamoto, K., Okumura, S. K., Ishizuki, S., & Scoville, N. Z. 1999, ApJS, 124, 403
- Sanders, D. B., Soifer, B. T., Elias, J. H., Madore, B. F., Matthews, K., Neugebauer, G., & Scoville, N. Z. 1988, ApJ, 325, 74
- Sanders, D. B., Mazzarella, J. M., Kim, D.-C., Surace, J. A., & Soifer, B. T. 2003, AJ, 126, 1607 (RBGS)
- Sheth, K., Vogel, S. N., Regan, M. W., Thornley, M. D., & Teuben, P. 2005, ApJ, 632, 217
- Smail, I., Ivison, R. J., & Blain, A. W. 1997, ApJ, 490, L5
- Siebenmorgen, R., Krügel, E., & Chini, R. 1999, A&A, 495
- Spergel, D. N., et al. 2003, ApJS, 148, 175
- Soifer, B. T., & Neugebauer, G. 1991, ApJ, 101, 354
- Soifer, B. T., Boehmer, L., Neugebauer, G., & Sanders, D. B. 1989, AJ, 98, 766
- Soifer, B. T., Sanders, D. B., Madore, B. F., Neugebauer, G., Danielson, G. E., Elias, J. H., Lonsdale, C. J., & Rice, W. L. 1987, ApJ, 320, 238
- Soifer, B. T., Sanders, D. B., Neugebauer, G., Danielson, G. E., Lonsdale, C. J., Madore, B. F., & Persson, S. E. 1986, ApJ, 303, L41
- Soifer, B. T., et al. 1984, ApJ, 278, L71
- Sopp, H. M., & Alexander, P. 1992, MNRAS, 259, 425

- Sopp, H. M., & Alexander, P. 1991, MNRAS, 251, 112
- Sprayberry, D., Impey, C. D., Bothun, G. D., & Irwin, M. J. 1995, AJ, 109, 558
- Stanford, S. A., Stern, D., van Breugel, W., & de Breuck, C. 2000, ApJSS, 131, 185
- Stickel, M., et al. 2000, A&A, 359, 865
- Tacconi, L. J. et al. 2006, ApJ, 640, 228
- Trewhella, M., Davis, J. I., Alton, P. B., Bianchi, S., & Madore, B. 2000, 543, 153
- Wang, Z., & Helou, G. 1992, ApJ, 398, L33 (WH)
- Young, J. S. 1999, ApJ, 514, L87
- Zink, E. C., Lester, D. F., Doppmann, G., & Harvey, P. M. 2000, ApJSS, 131,440

Table 1. Partial list of low luminosity star forming galaxies (SFGs)

Num.	Name	S_{12}	S_{25}	S_{60}	S_{100}	S_R	d	Flag	L_{TIR}	θ_M^B	θ_m^B	θ_M^{NIR}	θ_M^R	θ_m^R	θ_{beam}^R	Morp.
1	2	3	4	5	6	7	8	9	10	11	12	13	14	15	16	17
1	NGC4565 ^c	1.36	1.36	7.79	34.62	18.0	9.99	S	9.66	954.0	114.0	191.1	360.0	42.0	60.0	SA(s)b?
2	NGC3953 ^c	1.10	1.19	7.11	31.12	7.2	17.58	S	10.09	414.0	210.0	132.3	210.0	84.0	60.0	SB(r)bc
3	NGC5907 ^c	1.29	1.44	9.14	37.43	16.2	12.08	S	9.85	768.0	78.0	235.3	216.0	36.0	48.0	SA(s)c:
4	NGC3147 ^c	1.95	1.03	8.17	29.61	49.8	41.41	-	10.91	234.0	210.0	83.1	60.0	54.0	60.0	SA(rs)bc
5	NGC4579 ^c	1.12	0.78	5.93	21.39	62.9	15.29	V	9.87	354.0	282.0	120.0	54.0	24.0	54.0	SAB(rs)b
6	NGC0772 ^c	1.10	0.92	6.73	24.15	27.2	28.71	S	10.46	432.0	258.0	105.2	72.0	66.0	60.0	SA(s)b
7	NGC5371 ^c	0.86	0.97	5.27	18.66	10.3	41.06	-	10.67	264.0	210.0	102.4	120.0	96.0	54.0	SAB(rs)bc
8	NGC3675 ^c	1.43	1.67	10.48	36.56	17.2	12.69	S	9.92	354.0	186.0	120.7	84.0	36.0	48.0	SA(s)b
9	NGC4013 ^c	0.54	0.77	7.01	24.36	13.9	13.76	S	9.76	314.9	63.0	111.4	90.0	12.0	48.0	SAb
10	NGC4699 ^c	0.76	0.54	6.11	19.95	8.5	21.71	-	10.12	228.0	156.0	100.9	60.0	48.0	60.0	SAB(rs)b
11	NGC4501 ^c	2.29	2.98	19.68	62.97	73.7	15.29	V	10.33	414.0	222.0	155.4	120.0	66.0	54.0	SA(rs)b
15	NGC0908 ^c	1.74	2.21	17.54	52.35	35.8	15.75	S	10.27	360.0	156.0	128.9	90.0	66.0	48.0	SA(s)c
20	NGC5005 ^c	1.65	2.26	22.18	63.40	49.5	18.09	-	10.46	348.0	168.0	130.8	96.0	36.0	48.0	SAB(rs)bc
24	NGC3672 ^c	1.01	0.95	9.23	25.69	23.3	27.70	-	10.47	252.0	114.0	94.0	84.0	42.0	48.0	SA(s)c
25	NGC4030 ^c	1.35	2.30	18.49	50.92	66.5	24.50	-	10.64	252.0	180.0	77.4	72.0	60.0	60.0	SA(s)bc
140	NGC4102 ^w	1.77	6.83	46.85	70.29	46.1	16.89	-	10.61	162.0	60.0	68.6	3.3	2.2	1.5	SAB(s)b?
141	NGC7465 ^w	0.26	0.67	5.47	8.14	11.7	27.44	-	10.10	72.0	48.0	27.8	6.0	5.0	15.0	SB(s)0
142	NGC4383 ^w	0.29	1.08	8.36	12.43	4.8	15.29	V	9.76	114.0	60.0	35.0	8.0	5.0	5.0	SAa?
143	NGC4536 ^w	1.55	4.04	30.26	44.51	36.1	14.92	P	10.32	456.0	192.0	113.5	11.0	6.0	5.0	SAB(rs)bc
144	NGC3471 ^w	0.33	1.26	8.31	12.21	12.2	34.07	-	10.47	104.4	50.4	35.2	8.0	5.0	6.0	SAa
145	NGC5930 ^w	0.35	1.60	9.36	13.68	10.2	42.47	-	10.72	102.0	54.0	46.2	2.8	1.8	1.5	SAB(rs)b
146	NGC2798 ^w	0.76	3.21	20.60	29.69	9.9	27.84	-	10.69	156.0	60.0	38.7	4.5	1.6	1.5	SB(s)a
147	NGC1482 ^w	1.55	4.68	33.36	46.73	17.8	25.09	-	10.80	150.0	84.0	42.9	8.9	4.2	2.1	SA0+
148	NGC1204 ^w	0.25	1.10	7.33	10.18	14.2	58.51	-	10.88	66.0	18.0	33.3	1.9	1.0	1.8	S0/a:
149	NGC1022 ^w	0.71	3.28	19.71	27.33	26.4	19.33	-	10.35	144.0	120.0	56.3	4.0	3.0	6.0	SB(s)a
150	NGC3885 ^w	0.57	1.47	11.89	16.25	23.4	22.93	-	10.27	144.0	60.0	56.8	8.0	3.0	7.0	SAB(r:)0/a
151	NGC1266 ^w	0.25	1.20	13.13	16.89	75.7	28.86	-	10.46	90.0	60.0	32.8	5.0	2.0	6.0	SB(rs)0
152	NGC3597 ^w	0.67	2.18	12.84	16.21	34.8	48.31	-	10.97	114.0	90.0	25.0	8.0	5.0	7.0	S0+
153	NGC1222 ^w	0.50	2.28	13.06	15.41	43.8	32.26	-	10.60	66.0	54.0	22.9	11.0	7.0	18.0	S0-
154	NGC0839 ^w	0.52	2.27	11.67	13.03	15.1	51.10	-	10.97	84.0	42.0	29.2	2.6	1.3	1.8	SApec

Note. — *c* :cool; *w* :warm; θ_M :major axis; θ_m :minor axis
 Col.1 :Number; Col.2 :Galaxy Name; Col.s 3-6 :*IRAS* flux densities (Jy) from Revised Bright Galaxy Sample (RBGS; Sanders et al. 2003);
 Col.7 :1.49 *GHZ* flux density (mJy) (Peak flux S_P in Condon, Anderson & Helou 1991; Wang & Helou 1992) Col.8 : estimated galaxy
 distance d in Mpc; col.9 : flags P,S,V on distance estimate (see RBGS Table 1 for details); Col.10 :total IR luminosity $\log_{10}[L_{TIR}]$
 in L_{\odot} (RBGS); Col.s 11-12:*B*–band 25 mag arcsec⁻² major and minor axes (arcsec); Col.13 :*K_s* band 20 mag arcsec⁻² major axis
 (arcsec); Col.14-15 :1.49 *GHZ* major and minor axes for the resolution at which the galaxy is resolved (arcsec); Col.16 :1.49 *GHZ* beam
 resolution; Col.17 : Galaxy optical morphology.

Table 2. Correlation statistics from Pearson’s Correlation Test

Galaxy Class	$C - SB_R$		$C - D_R$		$C - D_{NIR}$		$C - D_B$	
	r	P	r	P	r	P	r	P
SFGs+LIRGs+ULIRGs	0.77	1.0E-08	-0.65	2.14E-07	-0.14	4.74E-02	-0.11	1.15E-01
SFGs+LIRGs	0.77	1.0E-08	-0.67	1.83E-08	-0.22	1.91E-03	-0.19	5.33E-03

Note. — Correlation statistics for FIR color C vs. all other parameters in Fig. 2. In this table, r is the correlation coefficient, and P is the probability that correlation could arise from an uncorrelated sample. The confidence is $1 - P$. Galaxy 1.49 GHz surface brightness and size are represented by SB_R and D_R . For both K_s and B bands, test is performed after removing galaxies with unknown sizes.